Journal of Microscopy, Vol. 202, Pt 1, April 2001, pp. 193–201.
Received 28 August 2000; accepted 11 October 2000

Low temperature near-field luminescence studies of localized and delocalized excitons in quantum wires

F. INTONTI*, V. EMILIANI*, C. LIENAU*, T. ELSAESSER*, R. NÖTZEL† AND K. H. PLOOG†
**Max-Born-Institut für Nichtlineare Optik und Kurzzeitspektroskopie, D-12489 Berlin, Germany*
†Paul-Drude-Institut für Festkörperelektronik, D-10117 Berlin, Germany

Key words. Excitons, low temperature near-field microscopy, luminescence spectroscopy, quantum wire.

Summary

Excitons in a GaAs quantum wire were studied in high-resolution photoluminescence experiments performed at a temperature of about 10 K with a spatial resolution of 160 nm and a spectral resolution of 100 μeV. We report the observation of quasi-one-dimensional excitons which are delocalized over a length of up to several micrometres along the quantum wire. Such excitons give rise to a 10 meV broad luminescence band, representing a superposition of transitions between different delocalized states. In addition, we find a set of sharp luminescence peaks from excitons localized on a sub150 nm length scale. Theoretical calculations of exciton states in a disordered quasi-one-dimensional potential reproduce the experimental results.

Introduction

The interplay between localized and delocalized electronic excitations underlies the fundamental optical and transport properties of low dimensional systems such as conjugated polymers (Pham *et al.*, 1995), electrons at surfaces (Ge *et al.*, 1998) and semiconductor nanostructures. In quasi-two-dimensional semiconductor quantum wells (QWs) and quasi-one-dimensional quantum wires (QWRs), the optical spectra in the range of the fundamental bandgap are determined by excitons showing a binding energy in the order of 10 meV which increases upon reducing the dimensionality of the semiconductor. In the simplest picture, neglecting any structural disorder in a QW or QWR, such excitons are fully delocalized in space. Modern epitaxial growth techniques allow us to fabricate in particular two-dimensional QW layers with ultrahigh, monolayer precision. During recent years, the optical properties of such samples have been the subject of intensive investigations. Many different experiments, e.g. resonance Rayleigh scattering studies, have shown that in many of such samples, localized excitons dominate their optical properties in the low excitation regime (Shchegrov *et al.*, 1999; Savona *et al.*, 2000). This exciton localization arises from slight spatial fluctuations in the bandgap potential that originate from structural imperfections of the material.

The recent progress in optical microprobing, in particular in the field of low-temperature near-field optical spectroscopy (NSOM), has allowed us to spatially and spectrally isolate the photoluminescence (PL) spectra from localized excitons in thin QWs (Hess *et al.*, 1994). These PL spectra are characterized by a set of sharp emission lines with linewidths between 10 and 100 μeV, when recorded with a submicrometre spatial resolution (Gammon *et al.*, 1996; Bonadeo *et al.*, 1998). The spectral envelopes and spatial properties of such line spectra which reflect a quasi-zero-dimensional behaviour of localized excitons depend largely on the length scale of interface roughness in the particular system and have been described by detailed theoretical models (Runge & Zimmermann, 1998; Larousserie, 1999; Savona *et al.*, 2000). So far, the role of delocalized exciton states in the QW spectra is less clear. Recent studies of thin QWs of substantial interface roughness by μ-PL suggest the occurrence of both types of excitons (Wu *et al.*, 1999).

Much less is known about the nanoscopic optical properties of quantum wires. A μ-PL study of T-shaped QWRs (Hasen *et al.*, 1997) suggests that at low temperatures and low excitation densities, the optical emission arises from closely spaced localized excitons. Evidence for delocalized excitonic states was not found and this makes these wires similar to a chain of quantum dots. Similar conclusions are drawn from recent studies of V-groove QWRs (Bellessa *et al.*, 1997; Vouilloz *et al.*, 1998).

In this paper, we study the luminescence properties of

Correspondence: Francesca Intonti. Tel: + 49 30 6392 1471; fax: + 49 30 6392 1489; e-mail: intonti@mbi-berlin.de

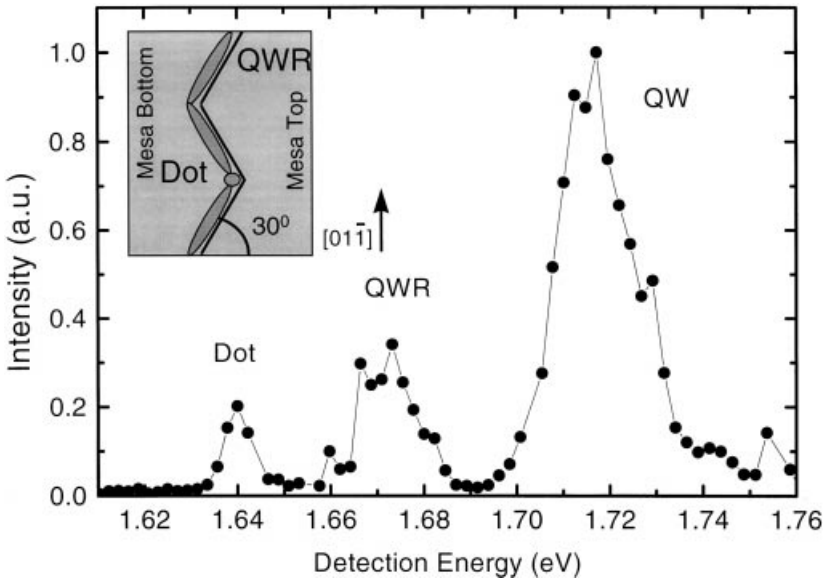

Fig. 1. Overview far-field photoluminescence spectrum ($T = 10$ K) of the coupled QWR-dot structure recorded near the corner of the sidewall intersection with a spatial resolution of about 3 μm. Inset: Schematic top view of the QWR-dot structure. The lithographic patterning of the substrate gives rise to the formation of a QWR along the sidewall and a dot at the corner of two intersecting sidewalls on the mesa top side.

single GaAs QWRs in a novel coupled QWR-dot nanostructure using low temperature near-field spectroscopy. The combination of high spatial resolution (160 nm) and high spectral resolution (100 μeV) allows us to resolve the characteristic emission features of excitons in a complex quasi-one-dimensional disorder potential. We demonstrate that localized excitons and excitons that are delocalized over a length of up to several microns along the QWR contribute to the QWR luminescence. Our experimental results are well reproduced by theoretical calculations of excitonic states in a disordered QWR.

Experimental

The experiments are performed with a home-built variable temperature near-field scanning optical microscope (Behme *et al.*, 1997) at temperatures between 10 K and 70 K. We operate the NSOM in an illumination/collection geometry, i.e. the excitation laser is transmitted through an NSOM fibre and the photoluminescence (PL) is collected back through the same fibre. PL spectra were recorded at each tip position with a $f = 50$ cm monochromator in conjunction with a cooled charge coupled device ($T = 77$ K, spectral resolution 100 μeV). Chemically etched single mode fibres (Lambelet *et al.*, 1998) with a taper angle of about 30° are taken as NSOM tips. These fibres are used without metal coating. As excitation sources serve either a HeNe laser (1.96 eV) or a tunable narrow-band Ti:sapphire laser (bandwidth < 200 μeV).

We investigate a GaAs/(AlGa)As coupled QWR-dot nanostructure grown by molecular beam epitaxy on a patterned GaAs (311)A substrate. On the substrate, a 15-nm high mesa with 4.5 μm long sidewalls alternately misaligned by ± 30° with respect to the [01−1] direction (zig-zag pattern) is prepared by wet chemical etching (Fig. 1, inset). The QWR structure consists of a nominally 3 nm thick GaAs QW layer clad between 50 nm $Al_{0.5}Ga_{0.5}As$ barriers. QWRs are formed due to the preferential migration of Ga ad-atoms from the mesa top and bottom towards the sidewalls of the mesa (Nötzel *et al.*, 1996). This results in a local increase of QW thickness up to 4.5 nm and a corresponding quasi-one-dimensional lateral confinement (Fricke *et al.*, 1999b). The Ga ad-atom migration is driven by the difference in ad-atom surface migration lengths between mesa top and bottom (long migration lengths) and sidewall planes (short migration length). Therefore the local increase in thickness in the QW plane at the mesa sidewall can be varied by changing the sidewall migration length.

It was recently demonstrated (Fricke *et al.*, 1999a) that such a variation can be achieved in a controlled way by changing the orientation of the sidewall plane. This approach is exploited in our sample for the formation of a coupled QWR-dot structure. Along the 4.5 μm long sidewalls the local increase in QW thickness is homogeneous and QWRs are formed. At the intersection of two QWR segments that points towards the mesa top (Fig. 1, inset), however, the change in sidewall orientation leads to a local increase in QW thickness, and thus to a local reduction in bandgap energy. Dots are formed at the end of the QWR segment and their emission is red shifted with respect to the QWR emission. The quasi-one-dimensional confinement potential of this type of QWR has been studied in earlier PL and PLE measurements (Richter *et al.*, 1997; Lienau *et al.*, 1998). From similar experiments, we conclude that in this structure the lateral width of the confined QWR region and the quasi-one-dimensional

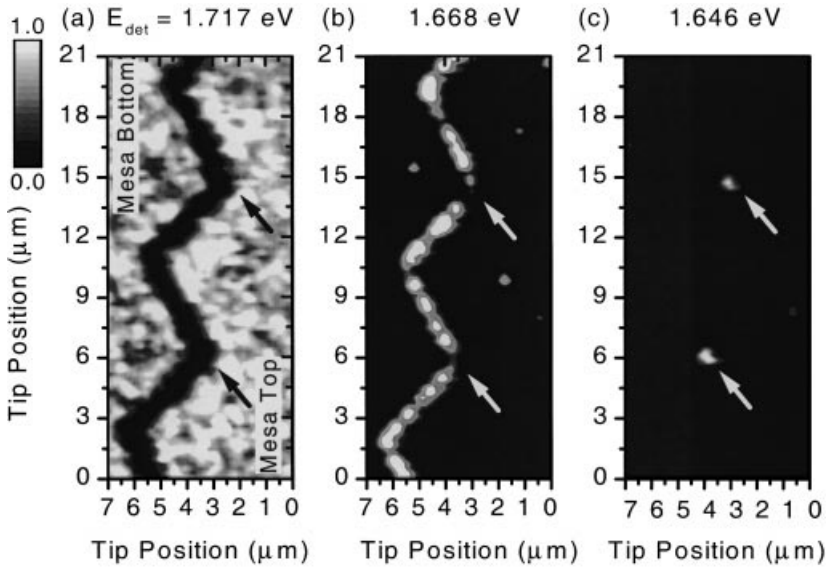

Fig. 2. Low temperature near-field images of the luminescence from the coupled QWR-dot sample recorded at three different detection energies E_{det} at $T = 10$ K in an illumination/collection geometry with a spectral resolution of 0.6 nm. (a) E_{det} = 1.717 eV (quantum well emission). (b) 1.668 eV (quantum wire emission). (c) 1.646 eV (dot emission).

confinement energy of excitons are 70 nm and 55 meV, respectively.

Experimental results

An overview far-field spectrum recorded with reduced spatial resolution and spectral resolution (0.6 nm) at a tip-to-sample distance of about 3 μm is shown in Fig. 1. The tip is positioned near the corner of the intersection of the two inclined sidewalls (Fig. 1, inset). Three major emission peaks at 1.640, 1.670 and 1.716 eV are clearly resolved. The spatial origin of these different peaks is revealed from near-field illumination/collection mode images recorded at different detection energies with a reduced spectral resolution of 0.6 nm (Fig. 2). Figure 2(a) shows that the peak at 1.716 eV arises from the homogeneous quantum well emission on both mesa top and bottom. For detection at 1.668 eV (Fig. 2(b)), we find along the entire length of the zigzag sidewalls a homogeneous QWR emission. There is a distinct reduction in emission intensity at the corner of the zigzag pattern that points towards the mesa top. Directly at the corners, intense luminescence with a maximum intensity that is about the same as that of the wire emission is observed at a detection energy of 1.646 eV (Fig. 2(c)). This dot-like emission is only found in a narrow spot with a diameter of less than 350 nm around the corner position. The optical spectra of the dot region will be discussed in detail elsewhere and we focus in the following on the QWR emission.

A line scan of the QWR PL (E_{det} = 1.668 eV) perpendicular to the QWR axis shows that in this experimental configuration the QWR luminescence is imaged with a spatial resolution of 160 nm (Fig. 3). The inset shows a plot of the data on a logarithmic intensity scale together with a Gaussian fit to the data (solid line) with a full width at half maximum (FWHM) of 160 nm. The high spatial resolution that is observed in this experimental configuration with uncoated tapered fibres with taper angles of about 30° is consistent with recent theoretical simulations (Müller & Lienau, 2000). It demonstrates that such uncoated probes combine high spatial resolution and very high emission and collection efficiencies. This makes such probes particularly interesting for the spectroscopy of subsurface semiconductor nanostructures.

As the combined spatial/spectral resolution is decreased below 200 nm/100 μeV, the broad QWR PL band breaks up into a set of sharp and intense emission peaks with spectral widths that range from 200 to 350 μeV (Fig. 4a). These sharp peaks are superimposed on a broad background emission. The near-field PL spectrum was recorded at a fixed position on the QWR. As the tip is scanned along the QWR, the spectral distribution of the sharp emission peaks fluctuates strongly, whereas a background emission is observed at all positions.

Two-dimensional near-field images, recorded at the spectral position of the sharp lines (Fig. 4(b)) show that these luminescence contributions stem from regions resolution-limited in size. Thus, they are attributed to the emission of localized excitons out of local potential minima that arise from monolayer-height fluctuations of the QWR profile (Hess *et al.*, 1994; Hasen *et al.*, 1997). When the detection energy is tuned to the low energy side of the broad continuum (out of the sharp resonances), the PL spatial distribution reveals the existence of regions with a larger average extension of 400–600 nm in diameter (Fig. 4c). For detection

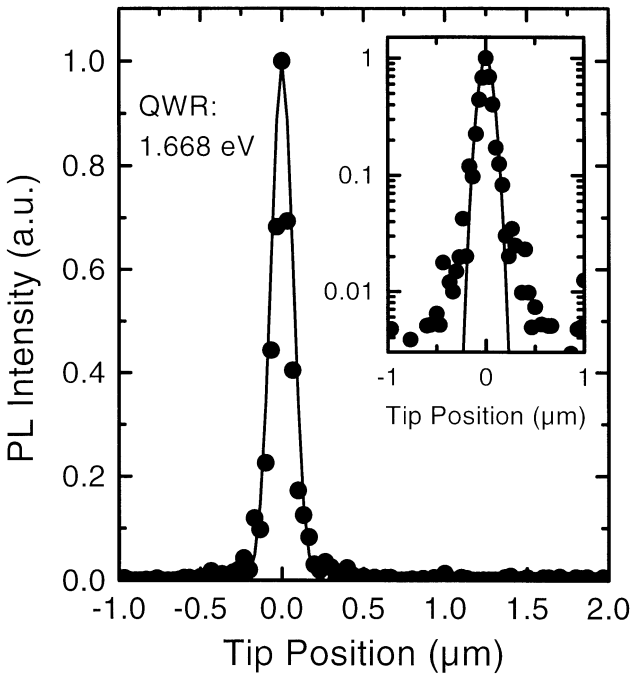

Fig. 3. Spatial resolution in illumination/collection geometry with uncoated etched fibre probes. Solid circles: spatial profile of the QWR luminescence ($E_{det} = 1.668$eV, $T = 10$ K). The tip is scanned along the y direction, perpendicular to the QWR axis. Solid line: Gaussian fit to the luminescence profile with a full width at half maximum (FWHM) of 160 nm. Inset. QWR luminescence on a logarithmic scale.

energies in the high energy part of the emission band, a completely different situation appears. Here, the two-dimensional images (Fig. 4d, detection at 1.674 eV, excitation at 1.96 eV), indicate a uniform PL distribution delocalized along the QWR axis on a length scale of more than 2 μm. An even larger extension is measured in the region where the QWRs are not interrupted by dots (Fig. 4e, excitation at 1.70 eV). In this case the spatial distribution of the PL signal extends over the whole QWR across the corner.

Such delocalized PL components are observed for a broad range of detection energies. The corresponding spectral dependence is shown in Fig. 4(a) by the dotted curve. The shape of this spectrum is close to a Gaussian centred at 1.6740 eV with a FWHM of 10 meV. Similar spectra were measured in different regions of the sample and are independent of the excitation photon energy in the range between 1.70 and 2 eV.

Figure 5 shows the power dependence of the near-field PL spectra recorded at a fixed position along the QWR. The excitation power was varied over more than three orders of magnitude with values between $P = 0.002$ μW and $P = 5.6$ μW, corresponding to carrier densities between 1.4×10^2 cm^{-1} and 4×10^5 cm^{-1}. We find that the intensity of the sharp peak emission increases roughly linearly with excitation density up to powers of about 2 μW. Note that the broad continuum contributes significantly to the PL spectra even at the lowest excitation density.

Temperature-dependent near-field spectra of the QWR emission are shown in Fig. 6 for temperatures between 10 and 70 K. Temperature-dependent QWR PL spectra recorded at a fixed spatial position are shown in Fig. 7. At the lowest temperatures, 10 K and 20 K, the emission from localized excitons is characterized by both spatially and spectrally narrow emission spikes. By counting the number of spectrally sharp spikes we estimate a density of about 7–10 μm^{-1}. As the temperature increases, these emission lines broaden spectrally. At the highest temperatures, the spectrum is transformed mainly into a broad, featureless emission band.

Discussion

The PL spectra of the QWR observed in our experiments reveal three emission components with distinctly different spectral and spatial features: (i) a set of spectrally sharp PL lines originating from individual strongly localized exciton sites with less than 150 nm diameter; (ii) a spectrally broader component with a spatial extension of about 500 nm; and (iii) emission from excitons which are delocalized along the QWR over a length of up to several micrometres and cover a 10 meV range of emission energies. This delocalized component is present even at very low excitation densities where only a minor fraction of the available exciton states in the QWR is populated and thus non-linear effects of state and/or band filling can safely be neglected.

The occurrence of the three PL components clearly demonstrates that disorder-induced local variations of the quasi-one-dimensional confinement potential of the QWR and the interplay between localized and delocalized states play a central role for the electronic properties of this type of QWR structure. We performed a theoretical study of the excitonic spectra in order to develop a quantitative understanding of the disordered QWR structure. In this model, we consider a QWR orientated along the *x*-axis with a lateral confinement potential V(y) of a width of 70 nm and a confinement energy of 55 meV, superimposed by a randomly generated potential (Fig. 8a). The random potential is characterized by a Gaussian energy distribution of width σ and a Gaussian correlation function in space of correlation length L_c. In the (x,y) plane, excitons are subject to local energy fluctuations both along the QWR axis (x) and perpendicular to it (y). Following the procedure outlined by Runge & Zimmermann (1998), the in-plane exciton centre-of-mass (COM) eigenenergies and wavefunctions $\psi(R)$ ($R = (X,Y)$: COM coordinate) are calculated by numerically solving the two-dimensional Schrödinger equation for the COM motion

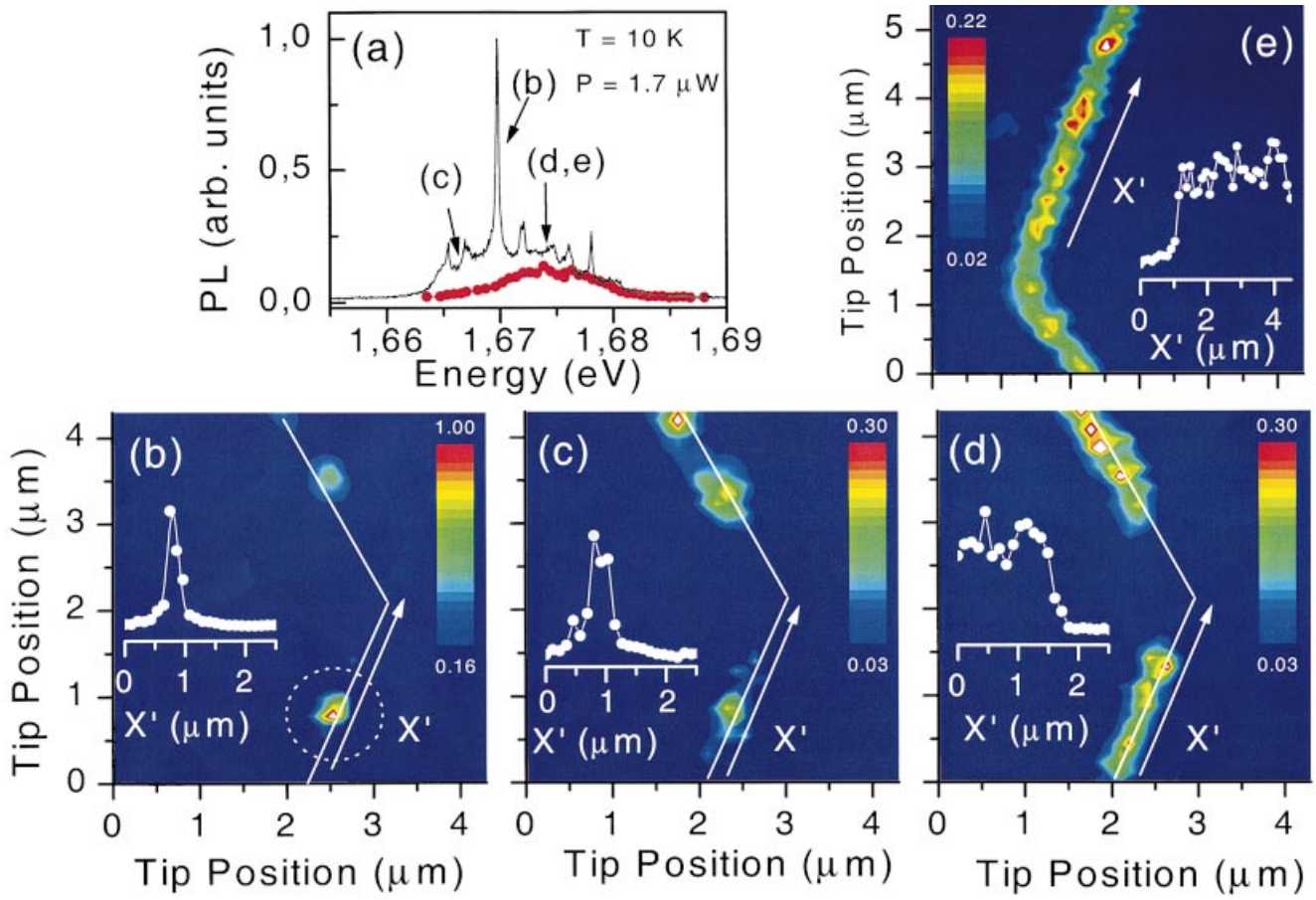

Fig. 4. (a) (Solid line) Near-field PL spectrum of the QWR taken at 10 K at a fixed tip position corresponding to (2.5 μm,0.5 μm) in Fig. 2(b–d). (Red circles) Spectral distribution of the spatially delocalized PL contribution. (b) Two dimensional near-field PL image taken at a fixed detection energy of $E_{det} = 1.6698$ eV (sharp emission peak in (a), excitation 1.96 eV) with a spectral resolution of 100 μeV. The spatial orientation of the QWR-dot structure is indicated as a solid line. Inset: Cross-section through the 2D image along the QWR axis X′. (c) Same as (b), with $E_{det} = 1.6643$ eV. (d) Same as (b) with $E_{det} = 1.674$ eV (delocalized PL component). (e) Near-field PL image taken at $E_{det} = 1.674$ eV (delocalized PL component) for excitation at 1.70 eV at a different spatial position on the sample covering a corner where two QWRs are not interrupted by dots.

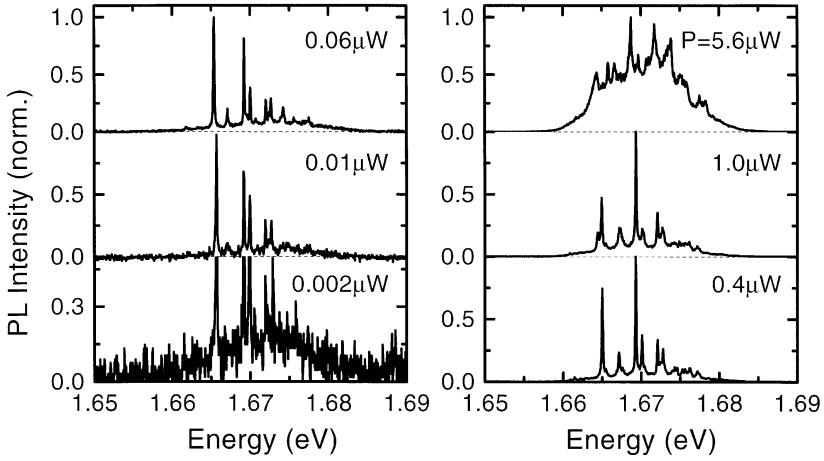

Fig. 5. Power dependence of the near-field QWR PL spectra taken at 10 K. The excitation power is varied between $P = 0.002$ μW and $P = 5.6$ μW. Note the broad continuum that contributes significantly to the PL spectra even at the lowest excitation density.

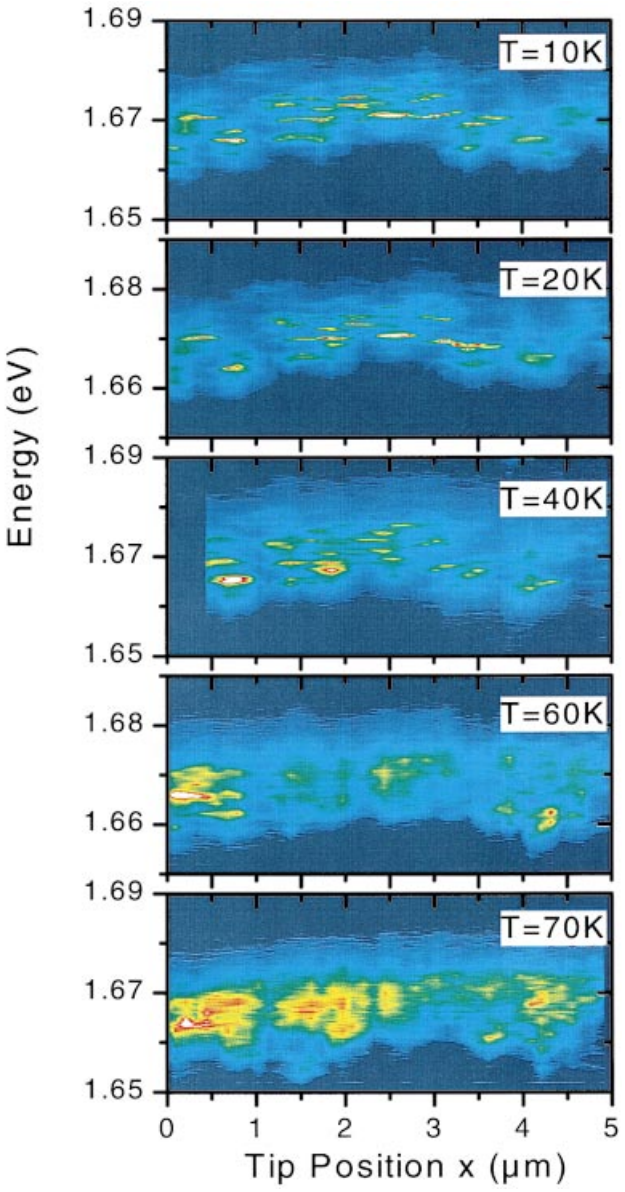

Fig. 6. Spatial variation of the QWR PL spectra for temperatures between 10 and 70 K. The tip is scanned in steps of 100 nm over a range of 5 μm along the QWR axis. At low temperatures the emission from localized excitons is clearly resolved as sharp, spectrally and spatially narrow emission spikes in the PL spectra. At higher temperatures, this emission is strongly spectrally broadened.

within the local potential. For a disorder strength of several meV that is typical for the considered thin semiconductor nanostructure, three types of 1 s exciton states are found in the QWR.

Excitons localized in a single potential minimum (Fig. 8b) with a nearly Gaussian shaped wavefunction $\psi(R)$. The extension of $\psi(R)$ is defined by L_c along the QWR axis (x) and by the lateral width of the potential minimum along y. These localized excitons couple strongly to light with a matrix element $M \propto D\int dR\psi(R)$ (D: optical dipole matrix element of the excitonic 1 s transition) and give rise to sharp emission peaks in the near-field spectra. The axial density of these localized excitons is about $1/4L_c$, and they are distributed over an energy range of roughly 2σ. Comparison with the average number and energy distribution of emission lines in Figs 4 and 5 allows us to approximate the free parameters of the model as $L_c = 20$ nm and $\sigma = 5$ meV.

At low transition energies, we find several eigenstates with wavefunctions that extend over few local potential minima, thus showing extensions between 50 and 200 nm (Fig. 5c). Their coupling to light is reduced with respect to that of localized excitons. Comparison to experiment indicates that this class of wavefunctions gives rise to the emission from localized regions extending beyond the spatial resolution of our experiment in the low energy part of the PL spectrum (Fig. 4c).

We find a large density of about 10 states/(μm*meV) that are delocalized along the QWR with wavefunction extensions between several 100 nm and several μm. A representative wavefunction with an extension of about 600 nm is shown in Fig. 8(d). The wavefunctions of these eigenstates show highly complex shapes which represent disorder-induced interferences between a broad distribution of plane waves with momentum K_x centred around an average $< K_x > 0$. The fraction of this distribution with momentum $K_x < K_{max} = E_x n/\hbar c$ (E_x: exciton transition energy, n: refractive index) couples to light and contributes to absorption and emission spectra with a matrix element M that is considerably reduced compared to that of localized exciton states (Citrin, 1993). In the optical spectra, these delocalized states give rise to a broad distribution of densely spaced weak resonances. If the linewidth of the individual resonances is broader than their energy separation, individual transitions are not resolved and broad structureless bands occur in the absorption and – for sufficient thermal population of emitting states – also in the PL spectrum. We attribute the spectrally broad and spatially delocalized luminescence in our near-field measurements (Fig. 4d,e) to those delocalized excitons.

In Fig. 8(e), the overall optical spectrum calculated from the model is summarized. The square of the transition moment $|M|^2$, proportional to the absorption coefficient, is plotted as a function of energy for both localized (components (i) and (ii)) and delocalized exciton states. In agreement with our experiments, we find a broad quasi-continuous contribution from transitions between delocalized states, superimposed by individual transitions between localized levels. Both contributions occur in a similar range of transition energies. In the luminescence spectra, the relative contribution from individual

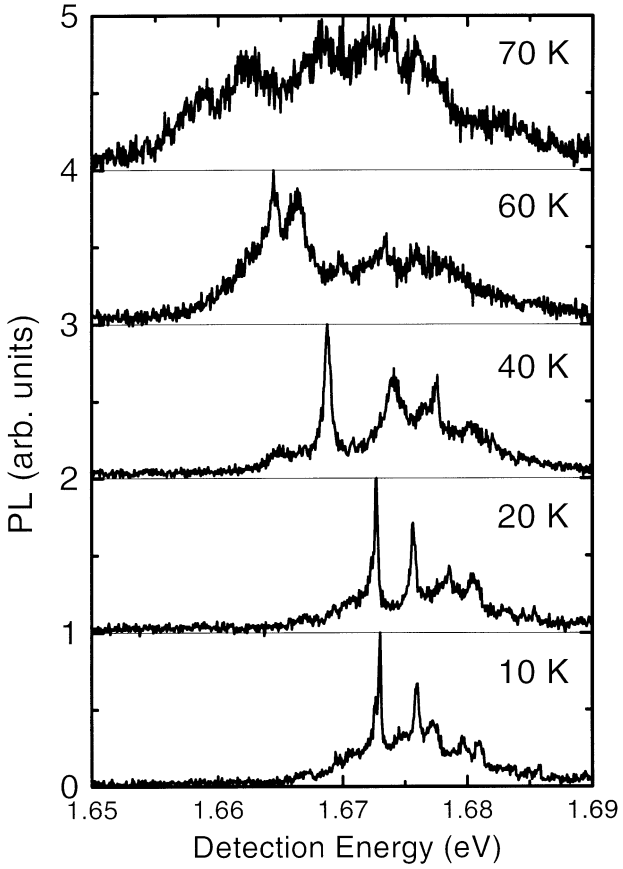

Fig. 7. Temperature dependent QWR PL spectra for temperatures between 10 and 70 K recorded at a fixed spatial position.

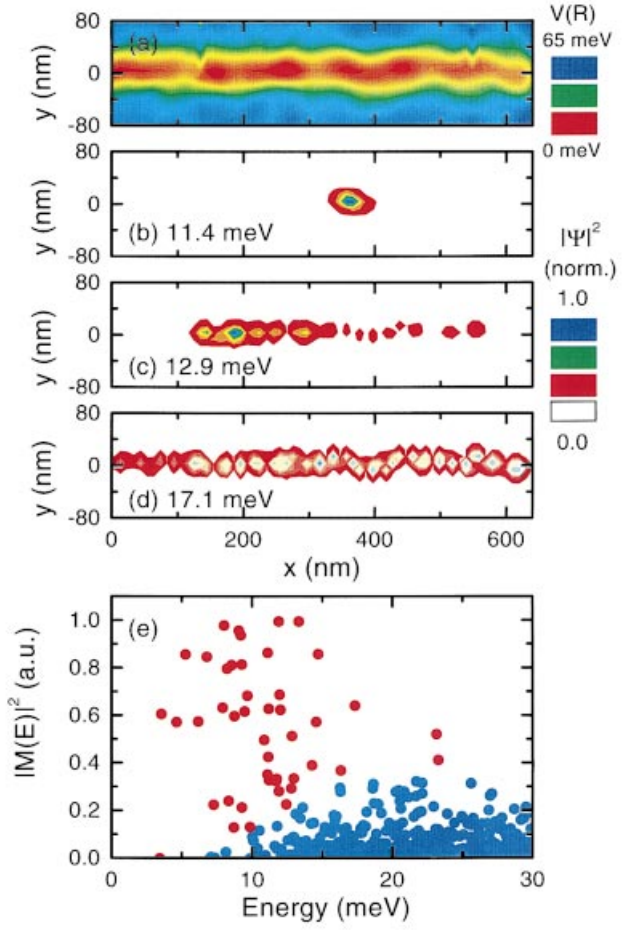

Fig. 8. (a) Potential distribution V(R = (x,y)) of the exciton COM potential of a disordered QWR along (x) and perpendicular (y) to the QWR axis. The confinement potential is taken as 55 meV with a lateral QWR width of 70 nm. The disorder potential is Gauss-correlated with $\sigma = 5$ meV and $L_C = 20$ nm. Probability densities $|\psi(R)|^2$ of representative (b) localized exciton wavefunctions, $E_X = 11.4$ meV, (c) weakly delocalized excitons, $E_X = 12.9$ meV, and (d) delocalized excitons, $E_X = 17.1$ meV. (e) Absorption spectrum calculated for a 2-μm long QWR. The different contributions from localized (○) and delocalized excitons (●) are highlighted.

eigenstates α is proportional to $|M_\alpha|^2 N_\alpha$, with N_α being the average occupation of α. In a quasi-equilibrium distribution of localized and delocalized excitons, N_α is determined by the energy of the exciton state and the temperature T_E of the exciton gas. The overall width of the measured delocalized PL component (circles in Fig. 4a) is well reproduced for a value of $T_E \sim 30$–40 K, i.e. somewhat higher than the lattice temperature of nominally 10 K. The elevated exciton temperature is due to the non-resonant excitation with excess energies of several 10 meV (see also Schnabel *et al.* 1992).

A comment should be made on the scattering processes underlying the luminescence linewidths. At low temperatures of the exciton gas, acoustic phonon scattering represents the main inelastic relaxation mechanism. A calculation of scattering matrix elements with the exciton wavefunctions derived in our model gives phonon emission times of 5–10 ps from delocalized exciton states for a lattice temperature of 10 K. This corresponds to characteristic line broadenings of 150–300 μeV. Such linewidths are larger than the energy separation between delocalized states, resulting in a broad structureless emission band as observed in our measurements. Phonon absorption times of localized excitons vary strongly between the different minima of the disorder potential. They are in the order of 10–30 ps at 10 K, corresponding to linewidths of 50–150 μeV, similar to what is found in the PL spectra. These acoustic phonon absorption rates increase linearly with increasing lattice temperature. This gives rise to a characteristic broadening of the localized exciton luminescence lines that is observed in the temperature range between 10 and 40 K (Figs 6 and 7). At higher temperatures the scattering of localized excitons out of their dot-like potential minima becomes so efficient that only a few individual emission lines are observable

and the PL spectrum transforms into a broad featureless emission band.

Conclusions

We have reported on a low temperature near-field luminescence study of a novel QWR-dot nanostructure. A combined spatial and spectral resolution of 160 nm and 100 μeV is obtained by choosing uncoated etched optical fibres as near-field tips. The high PL collection efficiency obtained with these probes in an illumination/collection geometry allowed us to resolve the characteristic emission features of excitons in complex quasi-one-dimensional disorder potential. The results evidence the coexistence of both localized and delocalized excitons in a quasi GaAs quantum wire. Excitons delocalized over a length of up to several micrometres give rise to a broad luminescence band. In contrast, excitons localized in minima of the quantum wire disorder potential lead to a set of narrow individual emission lines. Theoretical calculations of exciton states in a disorder potential account for this behaviour and show that the observed broad luminescence band consists of many individual transitions between delocalized states, each showing a spectral broadening larger than the mutual energy separation. Coupling between localized and delocalized states plays an important role for exciton relaxation and for excitonic transport along the quantum wire where contributions from both ballistic and diffusive motion are expected.

Acknowledgements

This work has been supported by the Deutsche Forschungsgemeinschaft (SFB296) and the European Union through the Ultrafast Quantum Optoelectronics Network, the EFRE program and a Marie-Curie Fellowship (ERB4001GT975 127) for one of the authors (V.E.). We gratefully acknowledge G. Cassabois for helpful discussions.

References

Behme, G., Richter, A., Süptitz, M. & Lienau, C. (1997) Vacuum near-field scanning optical microscope for variable cryogenic temperatures. *Rev. Sci. Instrum.* **68**, 3458.

Bellessa, J., Voliotis, V., Grousson, R., Wang, X.L., Ogura, M. & Matsuhata, M. (1997) High spatial resolution spectroscopy of a single V-shaped quantum wire. *Appl. Phys. Lett.* **77**, 2481–2483.

Bonadeo, N.H., Chen, G., Gammon, D., Katzer, D.S., Park, D. & Steel, D.G. (1998) Nonlinear nano-optics: probing one exciton at a time. *Phys. Rev. Lett.* **81**, 2759–2761.

Citrin, D.S. (1993) Radiative lifetimes of excitons in quantum wells. Localization and phase-coherence effects. *Phys. Rev. B* **47**, 3832–3841.

Fricke, J., Nötzel, R., Jahn, U., Niu, Z., Schönherr, H.-P., Ramsteiner, M. & Ploog, K.H. (1999a) Patterned growth on GaAs (311) A substrates: engineering of growth selectivity for lateral semiconductor nanostructures. *J. Appl. Phys.* **86**, 2896–2900.

Fricke, J., Nötzel, R., Jahn, U., Schönherr, H.-P., Däweritz, L. & Ploog, K.H. (1999b) Patterned growth on GaAs (311) A substrates: dependence on mesa misalignment and sidewall slope and its application to coupled wire-dot arrays. *J. Appl. Phys.* **85**, 3576–3581.

Gammon, D., Snow, E.S., Shanabrook, B.V., Katzer, D.S. & Park, D. (1996) Fine structure splitting in the optical spectra of single GaAs quantum dots. *Phys. Rev. Lett.* **76**, 3005–3008.

Ge, N.-H., Wong, C.M., Lingle,R.L.Jr, McNeill, J.D., Gaffney, K.J. & Harris, C.B. (1998) Femtosecond dynamics of electron localization at interfaces. *Science*, **279**, 202–205.

Hasen, J., Pfeiffer, L.N., Pinczuk, A., He, S., West, K.W. & Dennis, B.S. (1997) Metamorphosis of a quantum wire into quantum dots. *Nature*, **390**, 54–57.

Hess, H.F., Betzig, E., Harris, T.D., Pfeiffer, L.N. & West, K.W. (1994) Near-field spectroscopy of the quantum constituents of a luminescent system. *Science*, **264**, 1740–1745.

Lambelet, P., Sayah, A., Pfeffer, M., Philipona, C. & Marquis-Weible, F. (1998) Chemically etched fiber tips for near-field optical microscopy: a process for smoother tips. *Appl. Opt.* **37**, 7289–7292.

Larousserie, D. (1999) Relaxation de spin des excitons dans des hétérostructures de semiconducteurs. Doctoral thesis, Ecole Normale Supériere, Paris.

Lienau, Ch., Richter, A., Behme K.H. et al. (1998) Nanoscale mapping of confinement potentials in single semiconductor quantum wires by near-field optical spectroscopy. *Phys. Rev. B* **58**, 2045.

Müller, R. & Lienau, C. (2000) Propagation of femtosecond optical pulses through uncoated and metal-coated near-field fiber probes. *Appl. Phys. Lett.* **76**, 3367–3369.

Nötzel, R., Ramsteiner, M., Menniger, J., Trampert, A., . Schönherr, H.-P., Däweritz, L. & Ploog, K.H. (1996) Micro-photoluminescence study at room temperature of sidewall quantum wires formed on patterned GaAs (311) A substrates by molecular beam epitaxy. *Jpn. J. Appl. Phys.* **35**, L297–L300.

Pham, T.A., Daunois, A., Merle, J.-C., LeMoigne, J. & Bigot, J.Y. (1995) Dephasing dynamics of the vibronic states of epitaxial polydiacetelyne films. *Phys. Rev. Lett.* **74**, 904–908.

Richter, A., Behme, G., Süptitz, M. et al. (1997a) Real-space transfer and trapping of carriers into single GaAs quantum wires studied by near-field optical spectroscopy. *Phys. Rev. Lett.* **79**, 2145–2148.

Runge, E. & Zimmermann, R. (1998) Spatially resolved spectra, effectivie mobility edge, and level repulsion in narrow quantum wells. *Adv. Solid State Physics* **38**, 251–260.

Savona, V., Haacke, S. & Deveaud, B. (2000) Optical signatures of energy-level statistics in a disordered quantum system. *Phys. Rev. Lett.* **84**, 183–186.

Schnabel, R.F., Zimmermann, R., Bimberg, D., Nickel, H., Lösch, R. & Schlapp, W. (1992) Influence of exciton localization on recombination line shapes: $In_xGa_{1-x}As$/GaAs quantum wells as a model. *Phys. Rev. B* **46**, 9873–9876.

Shchegrov, A.V., Birkedal, D. & Shah, J. (1999) Monte Carlo

simulations of ultrafast resonant Rayleigh scattering from quantum well excitons: beyond ensemble averaging. *Phys. Rev. Lett.* **83**, 1391–1394.

Vouilloz, F., Oberli, D.Y., Lelarge, F., Dwir, B. & Kapon, E. (1998) Observation of many-body effects in the excitonic spectra of semiconductor quantum wires. *Solid State Comm.* **108**, 945–948.

Wu, Q., Grober, R.D., Gammon, D. &Katzer, D.S. (1999) Imaging spectroscopy of two-dimensional excitons in a narrow GaAs/AlGaAs quantum well. *Phys. Rev. Lett.* **83**, 2652–2655.